

Random site dilution properties of frustrated magnets on a hierarchical lattice

Jean-Yves Fortin

CNRS, Institut Jean Lamour, Département de Physique de la Matière et des Matériaux, UMR 7198, Vandoeuvre-les-Nancy, F-54506, France

E-mail: jean-yves.fortin@univ-lorraine.fr

Abstract. We present a method to analyze magnetic properties of frustrated Ising spin models on specific hierarchical lattices with random dilution. Disorder is induced by dilution and geometrical frustration rather than randomness in the internal couplings of the original Hamiltonian. The two-dimensional model presented here possesses a macroscopic entropy at zero temperature in the large size limit, very close to the Pauling estimate for spin-ice on pyrochlore lattice, and a crossover towards a paramagnetic phase. The disorder due to dilution is taken into account by considering a replicated version of the recursion equations between partition functions at different lattice sizes. An analysis at first order in replica number allows for a systematic reorganization of the disorder configurations, leading to a recurrence scheme. This method is numerically implemented to evaluate the thermodynamical quantities such as specific heat and susceptibility in an external field.

PACS numbers: 75.10.Hk, 05.50.+q, 75.10.Kt, 75.50.Lk

1. Introduction

Hierarchical lattices possess some interesting features of geometrical scale invariance, and several methods have been developed extensively in the past to study thermodynamical properties of spin models considered on such structures [1, 2]. The similarity with Migdal-Kadanoff renormalization procedure for magnetic spin systems [3] with exact recursion relations between coupling constants at the successive stages of lattice construction makes such models suitable for the study of critical properties. Indeed, phase transitions in these systems have non-mean field critical exponents, effective dimensions and frustration effects within local loops. However, the absence of translation and the site dependent connectivity inherent to such theoretical construction make the physics apparently different from real systems. The importance of exact solutions in disordered lattices are highlighted by the possibility to obtain controllable recursion relations which gives interesting properties for Ising spin glass and quenched disorder models [4, 5], or disordered Potts models [6]. Multicritical point locations can moreover be checked carefully using Nishimori symmetric lines [7, 8, 9] and duality exact properties [10]. Frustration on hierarchical lattices has been studied for example on a diamond shape ferromagnetic structure with an additional transverse antiferromagnetic coupling between two spins [11]. Important properties of the phase diagram when the coupling is increased concern the low temperature entropy which presents steps at specific values of this coupling reflecting the frustration character of the lattice geometry. These transitions are generated by slight variations of the transverse coupling inducing a change in the nature of the ground states. Recursion relations can be found exactly in this non-disordered but frustrated model, hence equations for ground state structure, residual entropy and magnetization can be obtained using scaling properties of the hierarchical geometry.

Experimental realizations of frustrated magnetic structures with spin dilution can be found in spin-ice materials doped with rare earth elements, such as $\text{Dy}_{2-x}\text{Lu}_x\text{Ti}_2\text{O}_7$, $\text{Dy}_{2-x}\text{Y}_x\text{Ti}_2\text{O}_7$, and $\text{Ho}_{2-x}\text{Y}_x\text{Ti}_2\text{O}_7$ [12], where x parametrizes the randomness [13]. These compounds are obtained from primary materials $\text{Dy}_2\text{Ti}_2\text{O}_7$ or $\text{Ho}_2\text{Ti}_2\text{O}_7$, where magnetic ions Dy^{3+} and Ho^{3+} occupy the sites of a pyrochlore lattice made of tetrahedra connected to each other by their vertices. The first magnetic rule for each individual tetrahedron is given by 2 spins out of the tetrahedron and 2 spins in, known as first ice rule [14]. These magnetic ions are then replaced by non-magnetic atoms Y or Lu, giving rise to an experimental system of site dilution where a macroscopic fraction of sites is non magnetic. One of the interesting physical properties of these systems is the non-monotonic behavior of the zero-temperature entropy with respect with the dilution level [13] from the measured specific heat, which can be explained quite accurately within the Pauling approximation where tetrahedra are treated as independent [13]. Refined calculations with Monte-Carlo simulations on Husimi cactus [15] is a step beyond the model of Pauling which takes into account the correlations between tetrahedra on the pyrochlore lattice [16]. In the Bethe-Peierls approximation, a tree-like structure

is constructed from a central site where the number of branches grows with the distance from the central site. However in this geometrical approach, the branches never reconnect together, a construction which forbids geometrical loops, but recursion equations can be in general written in a systematic manner. In this paper, we address the question of site disorder importance on thermal properties in the same spirit as [11] where frustration plays an important role.

We indeed consider explicitly an antiferromagnetic tetrahedron-like hierarchical structure with Ising spins $\sigma_i = \pm 1$ located on the vertices i . Disorder configurations are given by a set of additional quenched random variables $\epsilon_i = 0, 1$, with probability x and $(1 - x)$ respectively, located on the same sites (vertices) i , as shown in Fig. 1. The replicative procedure to construct iteratively the lattice is implemented starting from one single antiferromagnetic bond at level $r = 0$, until level $r > 0$ is reached, as exemplified on Fig. 1 for the first two steps. Such structure is known to have a well defined thermodynamical limit, when r is large, for the free energy per site [2, 17]. The zero temperature entropy of the tetrahedron-like structure at level $r = 1$ can be evaluated exactly as we will see in the next sections and it appears to be non-monotonic as function of the dilution. We can then generalize the calculation for larger structures $r > 1$ using recursion equations in the replica space, and obtain quantitative information about frustration and disorder effects in the thermodynamical limit. This simple model can be considered as a good example on how to characterize spin-ice or spin-liquid states and how these states may emerge for example from the specific heat or susceptibility measurements.

2. Notations and method

We consider the hierarchical lattice seen as a graph construction (set of vertices connected here by links or edges), build recursively an arbitrary number of times. Vertices can then be occupied by a spin with probability $(1 - x)$, with $0 \leq x \leq 1$, or stays vacant with probability x which is the dilution factor. Initially, at step $r = 0$, the graph consists of a single antiferromagnetic link, as displayed in Fig. 1(a), with two vertices occupied eventually by spins. This link has a Boltzmann strength $K = J/T$ with coupling unity $J = 1$. The structure at the next step is formed by replicating the previous structure four times, and by connecting the lower and upper vertices together, as in Fig. 1(b), (c) and in general (d). The diamond shape structures that are obtained are connected two by two to form a larger graph. Additionally, two transverse antiferromagnetic bonds of value $K' > 0$ [see Fig. 1 (b) (c) and (d)] are added at each step, in order to enhance frustration and to mimic tetrahedral structures. For example, step $r = 1$ is obtained by connecting four single edges to form a square, on which two antiferromagnetic edges of value K' are added transversely and longitudinally.

The spins considered in this paper are Ising spins $\sigma_i = \pm 1$ on each site (vertex) i , and we use an additional set of variables $\epsilon_i = 0$ when the spin is vacant, with probability x , or $\epsilon_i = 1$ when it is present with probability $1 - x$. It is straightforward to compute

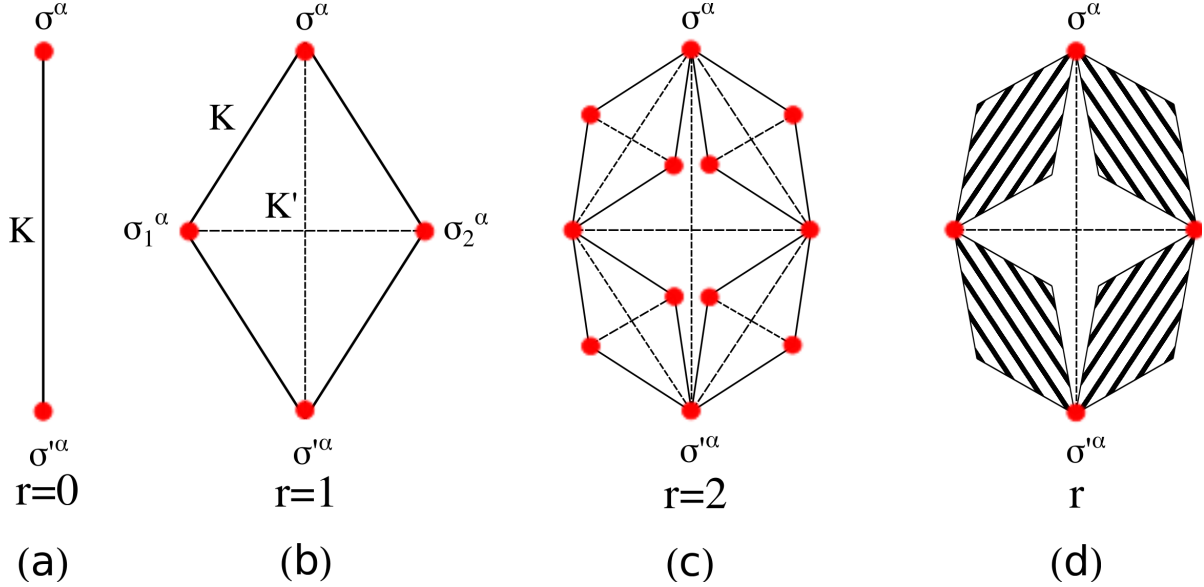


Figure 1. Construction of the hierarchical lattice, starting from a single link $K > 0$ between two spins (a). This link is replicated to form a diamond shape, and couplings $K' > 0$ are added successively between boundary sites, see (b) and (c), to form a frustrated lattice. Shaded areas in (d) defines the previous lattice structures at level $r - 1$, with bonds K' added furthermore between the boundary sites.

recursively the total number of vertices N_r at level r , equal to

$$N_0 = 2, N_1 = 4, N_{r+1} = 4N_r - 4, N_r = \frac{4^{r+1} + 8}{6}. \quad (1)$$

Also the total number of bonds B_r is equal to $B_r = 4^r + 2^{r+1} - 2$, and the maximum number of bonds connecting the two upper and lower sites is equal to $L_r = 2^r$. We may define an effective dimension d such that $B_r = L_r^d$, which gives $d = 2$ in the large size limit $r \gg 1$. In the following we will mainly concentrate on the frustrated case $K' = K$. Partition function for this dilute hierarchical lattice made of antiferromagnetic bonds can be constructed starting at step $r = 0$ using the following standard method. Also an external magnetic field h_e is taken into account in order to evaluate the spin susceptibility and magnetization.

After r recurrences, we define the partial partition function $Z_r^{\{\eta\}}(\epsilon\sigma, \epsilon'\sigma')$ which depends on some disorder configuration $\{\eta\}$ given by a set of vacancy distribution $\{\epsilon_i = 0, 1\}_i$ with i corresponding to the sites located inside the structure delimited by the two extreme sites $(\epsilon\sigma, \epsilon'\sigma')$. These latter sites have a given disorder configuration $\{\epsilon, \epsilon'\}$ which does not belong to $\{\eta\}$. A recursion relation can be written between steps r and $r + 1$ of the lattice construction

$$\begin{aligned} Z_{r+1}^{\{\eta\}}(\epsilon\sigma, \epsilon'\sigma') &= \text{Tr} \sigma_1, \sigma_2 Z_r^{\{\eta_1\}}(\epsilon\sigma, \epsilon_1\sigma_1) Z_r^{\{\eta_2\}}(\epsilon_1\sigma_1, \epsilon'\sigma') Z_r^{\{\eta_3\}}(\epsilon\sigma, \epsilon_2\sigma_2) Z_r^{\{\eta_4\}}(\epsilon_2\sigma_2, \epsilon'\sigma') \\ &\times \exp(-K'\epsilon_1\sigma_1\epsilon_2\sigma_2 + \frac{h_e}{T}(\epsilon_1\sigma_1 + \epsilon_2\sigma_2)) \times \exp(-K'\epsilon\sigma\epsilon'\sigma') 2^{\epsilon_1-1} 2^{\epsilon_2-1} \quad (2) \end{aligned}$$

where $\{\eta\}$ represents the disorder configuration $\{\eta\} = \{\eta_1, \eta_2, \eta_3, \eta_4, \epsilon_1, \epsilon_2\}$ and the Tr . sign the sum over all the possible spin values. The additional factors $2^{\epsilon_1-1}2^{\epsilon_2-1}$ compensate the fact that we sum over eventual ghost spins located on vacant sites. The initial condition Fig. 1(a) is given by the two-spin partition function

$$Z_0^{\{\eta\}}(\epsilon\sigma, \epsilon'\sigma') = \exp(-K\epsilon\epsilon'\sigma\sigma') \quad (3)$$

which has actually no internal disorder dependence, $\{\eta\} = \{\emptyset\}$. The magnetic field is implemented in (2) only for spins not belonging to the top and bottom vertices. Using replica method, we consider n copies of (2) for a given configuration $\{\eta\}$ and perform the average

$$Z_{r+1}(\epsilon\sigma^\alpha, \epsilon'\sigma'^\alpha) := \left[\prod_{\alpha=1}^n Z_{r+1}^{\{\eta\}}(\epsilon\sigma^\alpha, \epsilon'\sigma'^\alpha) \right]_\eta \quad (4)$$

Here $[\cdot]_\eta$ is meant for averaging over disorder $\{\eta\}$. In this case, the recursion relation (2) becomes

$$\begin{aligned} Z_{r+1}(\epsilon\sigma^\alpha, \epsilon'\sigma'^\alpha) &= \exp(-K'\epsilon\epsilon' \sum_{\alpha} \sigma^\alpha \sigma'^\alpha) \int P(\epsilon_1)P(\epsilon_2)d\epsilon_1d\epsilon_2 \text{Tr} \sigma_1^\alpha, \sigma_2^\alpha \\ &\times Z_r(\epsilon\sigma^\alpha, \epsilon_1\sigma_1^\alpha) Z_r(\epsilon_1\sigma_1^\alpha, \epsilon'\sigma'^\alpha) Z_r(\epsilon\sigma^\alpha, \epsilon_2\sigma_2^\alpha) Z_r(\epsilon_2\sigma_2^\alpha, \epsilon'\sigma'^\alpha) \\ &\times \exp \left[-K'\epsilon_1\epsilon_2 \sum_{\alpha} \sigma_1^\alpha \sigma_2^\alpha + \frac{h_e}{T} \sum_{\alpha} (\sigma_1^\alpha + \sigma_2^\alpha) \right] 2^{n(\epsilon_1-1)} 2^{n(\epsilon_2-1)} \end{aligned} \quad (5)$$

where P is the bimodal distribution for the dilute sites $P(\epsilon) := x\delta(\epsilon) + (1-x)\delta(\epsilon-1)$. In the previous expression, we perform only the sum over the two spins σ_1^α and σ_2^α connecting pairs of diamond shape structures. Starting with initial condition

$$Z_0(\epsilon\sigma^\alpha, \epsilon'\sigma'^\alpha) = \exp(-K\epsilon\epsilon' \sum_{\alpha} \sigma^\alpha \sigma'^\alpha) \quad (6)$$

all quantities $Z_r(\epsilon\sigma^\alpha, \epsilon'\sigma'^\alpha)$ can in principle be computed step by step. Free energy $F^{(r)}$ is evaluated directly after averaging over the remaining disorder and summation over the two spin variables. We define the complete partition function as

$$z_r(n) = \int P(\epsilon)P(\epsilon')d\epsilon d\epsilon' 2^{n(\epsilon-1)} 2^{n(\epsilon'-1)} \text{Tr} \sigma^\alpha, \sigma'^\alpha Z_r(\epsilon\sigma^\alpha, \epsilon'\sigma'^\alpha) \exp \left[\frac{h_e}{T} \sum_{\alpha} (\sigma^\alpha + \sigma'^\alpha) \right] \quad (7)$$

and take the limit $n \rightarrow 0$

$$-KF^{(r)} := \lim_{n \rightarrow 0} \frac{1}{n} (z_r(n) - 1) = z'_r(0) \quad (8)$$

after noticing that $z_r(0) = 1$. The disorder averaged entropy can be expressed in terms of $z'_r(0)$ via the usual thermodynamical relations

$$S^{(r)}(T) := -\frac{\partial F^{(r)}}{\partial T} = z'_r(0) - K \frac{\partial}{\partial K} z'_r(0) \quad (9)$$

as well as the averaged specific heat $C_v^{(r)} = -T \partial^2 F^{(r)} / \partial T^2 = K^2 \partial^2 z'_r(0) / \partial K^2$. The relation between entropy and specific heat is given by the integral

$$S^{(r)}(T) = N_r(1-x) \ln(2) - \int_T^\infty \frac{C_v^{(r)}}{T'} dT' \quad (10)$$

which is a direct experimental way to measure the zero-temperature entropy by extrapolation, knowing that all spins are in the paramagnetic phase at high temperature, each contributing with a factor $\ln(2)$. The linear susceptibility corresponds to the excitation of the magnetic order parameter $M = \sum_i \sigma_i$ under a field h_e and is defined as $\chi^{(r)} = \partial[\langle M \rangle]_\eta / \partial h_e$, after averaging over disorder. We can also relate $\chi^{(r)}$ to the free energy, using $T\chi^{(r)} = [\langle M^2 \rangle]_\eta - [\langle M \rangle^2]_\eta$ and $[\langle M \rangle]_\eta = -\partial F^{(r)} / \partial h_e$, in particular

$$\chi^{(r)} = \frac{\partial[\langle M \rangle]_\eta}{\partial h_e} = -\frac{\partial^2 F^{(r)}}{\partial h_e^2}. \quad (11)$$

3. Residual entropy for $r = 1$ structure

As a simple application, we consider the case $r = 1$ consisting in only 4 spins Fig. 1(b), where all thermodynamical quantities can be computed exactly. The zero temperature entropy is identical to the entropy of a three-dimensional tetrahedron made of antiferromagnetic bonds. After iterating (5), we obtain

$$\begin{aligned} Z_1(\epsilon\sigma^\alpha, \epsilon'\sigma'^\alpha) &= \exp(-K'\epsilon\epsilon' \sum_\alpha \sigma^\alpha \sigma'^\alpha) \times \\ &\left[(1-x)^2 2^n \prod_{\alpha=1}^n \left(e^{K'} + e^{-K'} \cosh \left[2K(\epsilon\sigma^\alpha + \epsilon'\sigma'^\alpha) - 2\frac{h_e}{T} \right] \right) \right. \\ &\left. + 2x(1-x) 2^n \prod_{\alpha=1}^n \cosh \left[K(\epsilon\sigma^\alpha + \epsilon'\sigma'^\alpha) - \frac{h_e}{T} \right] + x^2 \right]. \end{aligned} \quad (12)$$

Then the function $z_1(n)$ is equal, after some computation, to

$$\begin{aligned} z_1(n) &= (1-x)^4 4^n \left[1 + \left\{ \cosh(4K) + e^{-4K} \sinh^2\left(2\frac{h_e}{T}\right) \right\} e^{-2K'} + e^{2K'} + \cosh\left(2\frac{h_e}{T}\right) \right]^n \\ &\quad + 4x(1-x)^3 4^n \left[\cosh\left(\frac{h_e}{T}\right) e^{K'} + \left\{ \cosh(2K) \cosh\left(\frac{h_e}{T}\right) \cosh\left(2\frac{h_e}{T}\right) \right\} \right]^n \end{aligned}$$

$$\begin{aligned}
 & - \sinh(2K) \sinh\left(\frac{h_e}{T}\right) \sinh\left(2\frac{h_e}{T}\right) \left. \right\} e^{-K'} \Big]^n \\
 & + 2x^2(1-x)^2 2^n \left[\left(\cosh\left(2\frac{h_e}{T}\right) e^{-K'} + e^{K'} \right)^n + 2 \left(\cosh\left(2\frac{h_e}{T}\right) e^{-K} + e^K \right)^n \right] \\
 & + 4x^3(1-x) 2^n \cosh^n\left(\frac{h_e}{T}\right) + x^4.
 \end{aligned} \tag{13}$$

When K is large and in absence of external field, this expression can be put into the following form, by keeping the dominant contributions in the exponential terms

$$z_1(n) = \sum_{k \geq 0} \rho_k e^{n(s_k - K e_k)}, \quad \sum_{k \geq 0} \rho_k = 1. \tag{14}$$

This expansion is useful in order to identify the zero temperature entropy which can be written as a sum of contributions $S^{(1)}(T=0) = \sum_k \rho_k s_k$. Each partial entropy s_k and energy e_k physically corresponds to a configuration of disorder with weight ρ_k . In this limit, the asymptotic form for $z_1(n)$ when $0 \leq K' < K$ is indeed equal to

$$\begin{aligned}
 z_1(n) & \simeq (1-x)^4 2^n e^{n(4K-2K')} + 4x(1-x)^3 2^n e^{n(2K-K')} \\
 & + 4x^2(1-x)^2 2^n e^{nK} + 2x^2(1-x)^2 2^n e^{nK'} + 4x^3(1-x) 2^n + x^4.
 \end{aligned} \tag{15}$$

After taking the limit $n \rightarrow \infty$, the entropy and energy per spin are respectively equal to $S^{(1)}(T=0)/[4(1-x)] = (1-x^4)/[4(1-x)] \ln(2)$ and $E^{(1)}/[4(1-x)] = -(1-x)^3(1-\gamma/2) - x(1-x)^2(2-\gamma) - x^2(1-x)(1+\gamma/2)$, where $\gamma := K'/K$ is the coupling ratio. The frustrated case $K' = K$ is particular since we obtain instead

$$\begin{aligned}
 z_1(n) & \simeq (1-x)^4 6^n e^{n2K} + 4x(1-x)^3 6^n e^{nK} + 6x^2(1-x)^2 2^n e^{nK} \\
 & + 4x^3(1-x) 2^n + x^4
 \end{aligned} \tag{16}$$

and, in this specific case, the entropy and energy per spin have a different expression

$$\begin{aligned}
 \frac{S^{(1)}(T=0)}{4(1-x)} & = (1-x)^3 \frac{\ln(6)}{4} + x(1-x)^2 \ln(6) + 3x^2(1-x) \frac{\ln(2)}{2} + x^3 \ln(2), \\
 \frac{E^{(1)}(T=0)}{4(1-x)} & = -\frac{1}{2}(1-x)^3 - x(1-x)^2 - \frac{3}{2}x^2(1-x).
 \end{aligned} \tag{17}$$

As expected, the entropy for a single tetrahedron in the frustrated case is larger. Plot of the entropy is given in Fig. 5 as function of x and appears to be non-monotonic with a local maximum around $x = 0.295$. This maximum, intrinsic to a 4 spin system or single uncoupled tetrahedra, is probably due to the non-monotonic variation of the fraction of the spin configurations with the lowest energy as function of dilution in a system of 4 spins where there are at most 16 possible states, in a similar way as it is describes in [13] for coupled tetrahedra. This maximum disappears for $r > 1$ as shown

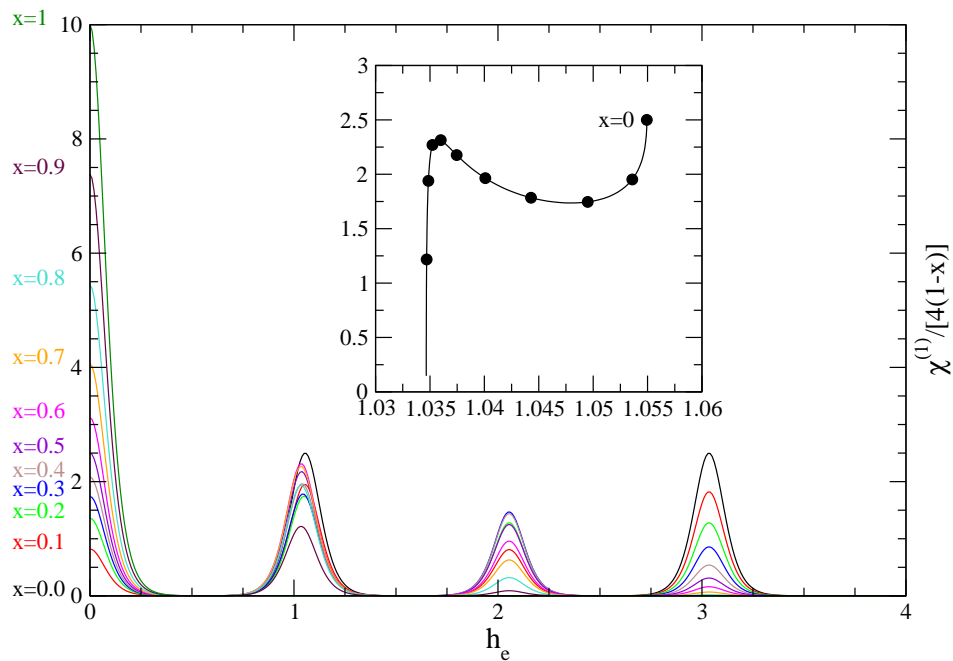


Figure 2. (Color online) Susceptibility per spin $\chi^{(1)}/[4(1-x)]$ at $T = 0.1$ as function of the external field h_e , for different values of dilution factor. In absence of disorder (black lines), the susceptibility is composed of two peaks located at $h_e = 1, 3$. Inset: variation of the second peak position with dilution.

on the same figure because the varying connectivity and coupling arrangement on the hierarchical structure tends to modify the fractions of these acceptable states in the different tetrahedral units. The exact entropy value in absence of dilution is given by $\ln(6)/4 \simeq 0.4479$ which is larger than for a system of coupled tetrahedra in the large size limit (see sections below).

Susceptibility $\chi^{(1)}$ is derived exactly using definition (11) and is plotted in Fig. 2 as function of the external field for different values of x . As expected, when $x > 0$, a peak appears at $h_e = 0$ when the probability to find a single spin in the tetrahedron is non zero. A simple calculation for the non-disordered case leads to three possible ground states per spin E_G depending on the value of the field: two spins up and two spins down with $E_G = -2$, three spins up and one spin down with $E_G = -2h_e$, and all spins up with $E_G = 6 - 4h_e$. Two transitions occur respectively at $h_e = 1$ and $h_e = 3$.

For larger sizes however, it is interesting to analyze the susceptibility using recursive equations (5) for the partition function $Z_r(\sigma, \sigma')$ in the absence of disorder $x = 0$. The recursive equations are detailed in Appendix A. The method is to assume an effective form for the partition function, with Ising effective coupling, magnetic field, and weight coefficient at all recursion levels. The exact recurrence equations for these three quantities as function of the external magnetic field h_e allow us directly to compute the susceptibility. Plots of $\chi^{(r=6)}(h_e)$ and magnetization per spin $m^{(r=6)}(h_e)$ are displayed in Fig. 3 showing multiple field transitions and magnetization plateaus up to $h_e = 127$ for $N_6 = 2732$ spins. In the next section, the analysis is extended to the dilute case. We

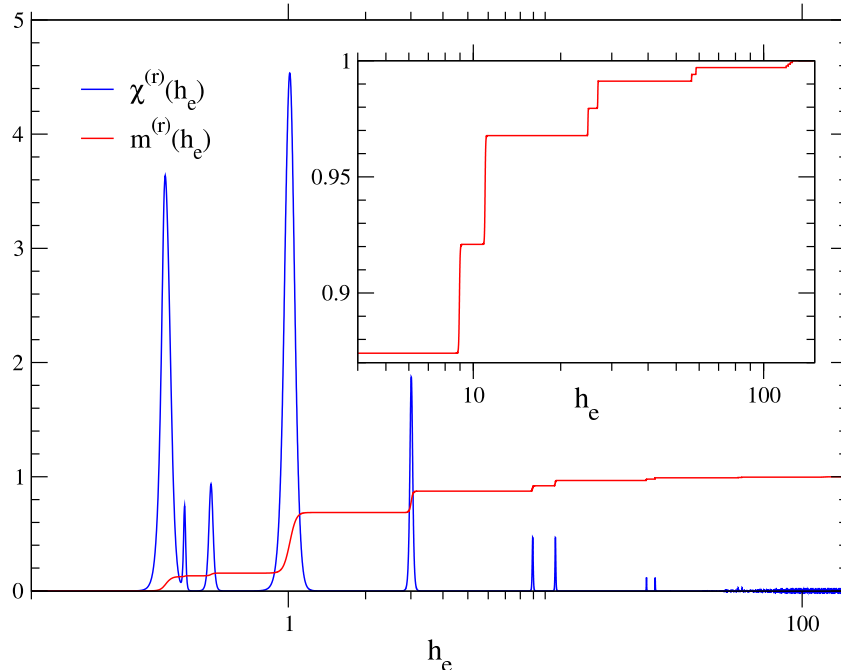


Figure 3. (Color online) Susceptibility (blue line) $\chi^{(r)}(h_e)$ and magnetization $m^{(r)}(h_e)$ (red line) per spin at $T = 0.05$ as function of the external field h_e (logarithmic scale) in absence of disorder for level $r = 6$ (2732 sites). Inset: magnetization per spin in the large field limit until saturation.

use the set of recursive equations (5) to compute the partition function at a given step r . The main technique is to reorganize the partition function in the same manner as (16) where we easily identify weights $\rho_k = x^k(1-x)^{4-k}C_4^k$. One difficulty with dilution is that an iterative procedure at low temperature on effective Ising constant couplings to obtain the limiting coupling distribution can in principle be performed, but not for the free energy, unlike the case of spin glass models. For example, for the disordered Potts model [6] where the disorder is given by a discrete distribution of couplings, zero temperature free energy satisfies some recursive equations. In general, when the disorder is located only in the couplings, the four structures represented as shaded areas in Fig. 1(c) have independent internal disorder, even if they are connected together by the four vertices. Therefore disorder can be factorized and direct iteration of Ising couplings by renormalization can be performed as well as the partition function weights such as I_r in (A.1) which are important for the determination of free energy and entropy. In the case of dilution however, the disorder configuration in the boundary vertex sites given by set $\{\epsilon, \epsilon', \epsilon_1, \epsilon_2\}$ is actually shared between the four diamond structures. For example variable ϵ_1 is common to the two shaded diamonds on the left hand side of Fig. 1(c). This makes the evaluation of weight coefficients I_r (A.1) problematic in the

disordered case since after few iterations correlations will develop rapidly. This is main reason why it is more convenient to consider a replica version of (A.1) and (2) with partial integration over the disorder located strictly inside the diamond structures, as explicitly defined previously by (5). As we will see, an approximation scheme can be derived from the replica method and thermodynamical functions can be obtained.

4. Recursion relations in the general case

At step r , we assume from the previous analysis an expansion of the partition function in terms of configurational weights $x^k(1-x)^{n_r-k}C_{n_r}^k$ where n_r is here the number of sites localized between the two extreme top and bottom sites and which satisfies the equation $n_{r+1} = 4n_r + 2$, with initial condition $n_0 = 0$ and $N_r = n_r + 2$. The main idea, as discussed before, is to keep a generic and minimal expression for the partial partition function, which depends on unknown functions satisfying recurrence equations such that

$$Z_r(\epsilon\sigma^\alpha, \epsilon'\sigma'^\alpha) = \exp(-K'\epsilon\epsilon' \sum_{\alpha} \sigma^\alpha \sigma'^\alpha) \sum_{k=0}^{n_r} x^k(1-x)^{n_r-k} C_{n_r}^k \exp\left(nI_k^{(r)}(\epsilon, \epsilon') + K_k^{(r)}\epsilon\epsilon' \sum_{\alpha} \sigma^\alpha \sigma'^\alpha + H_k^{(r)}(\epsilon, \epsilon') \sum_{\alpha} [\epsilon\sigma^\alpha + \epsilon'\sigma'^\alpha]\right) \quad (18)$$

where $H_k^{(r)}(\epsilon, \epsilon')$ and $I_k^{(r)}(\epsilon, \epsilon')$ are symmetric functions of ϵ and ϵ' . Coupling $K_k^{(r)}$ is independent of the boundary disorder. All these functions depend implicitly on K and h_e . As initial condition we impose $K_0^{(0)} = -K + K'$ and $H_0^{(0)}(\epsilon, \epsilon') = I_0^{(0)}(\epsilon, \epsilon') = 0$. We also take $K' = K$ in the following for the frustrated version. At the next level, Z_{r+1} is evaluated by considering the product of four partition functions Z_r as written in (5).

Using the ansatz (18), this product is expanded as

$$\begin{aligned} Z_{r+1} &= \exp(-K'\epsilon\epsilon' \sum_{\alpha} \sigma^\alpha \sigma'^\alpha) \sum_{k_1, k_2, k_3, k_4=0}^{n_r} C_{n_r}^{k_1} C_{n_r}^{k_2} C_{n_r}^{k_3} C_{n_r}^{k_4} x^{k_1+k_2+k_3+k_4} (1-x)^{4n_r-k_1-k_2-k_3-k_4} \\ &\times \int P(\epsilon_1)P(\epsilon_2)d\epsilon_1d\epsilon_2 \text{Tr} \sigma_1^\alpha, \sigma_2^\alpha \exp\left(nI_{k_1}^{(r)}(\epsilon, \epsilon_1) + nI_{k_2}^{(r)}(\epsilon_1, \epsilon') + nI_{k_3}^{(r)}(\epsilon, \epsilon_2) + nI_{k_4}^{(r)}(\epsilon_2, \epsilon')\right) \\ &\times \exp\left(-K'\epsilon_1\epsilon_2 \sum_{\alpha} \sigma_1^\alpha \sigma_2^\alpha - K' \sum_{\alpha} (\epsilon_1\sigma_1^\alpha + \epsilon_2\sigma_2^\alpha)(\epsilon\sigma^\alpha + \epsilon'\sigma'^\alpha)\right) 2^{n(\epsilon_1-1)} 2^{n(\epsilon_2-1)} \\ &\times \exp\left(K_{k_1}^{(r)}\epsilon\epsilon_1 \sum_{\alpha} \sigma^\alpha \sigma_1^\alpha + K_{k_2}^{(r)}\epsilon_1\epsilon' \sum_{\alpha} \sigma_1^\alpha \sigma'^\alpha + K_{k_3}^{(r)}\epsilon\epsilon_2 \sum_{\alpha} \sigma^\alpha \sigma_2^\alpha + K_{k_4}^{(r)}\epsilon_2\epsilon' \sum_{\alpha} \sigma_2^\alpha \sigma'^\alpha\right) \\ &\times \exp\left(H_{k_1}^{(r)} \sum_{\alpha} [\epsilon\sigma^\alpha + \epsilon_1\sigma_1^\alpha] + H_{k_2}^{(r)} \sum_{\alpha} [\epsilon'\sigma'^\alpha + \epsilon_1\sigma_1^\alpha] + H_{k_3}^{(r)} \sum_{\alpha} [\epsilon\sigma^\alpha + \epsilon_2\sigma_2^\alpha] + H_{k_4}^{(r)} \sum_{\alpha} [\epsilon'\sigma'^\alpha + \epsilon_2\sigma_2^\alpha]\right) \\ &\times \exp\left[\frac{h_e}{T} \sum_{\alpha} (\epsilon_1\sigma_1^\alpha + \epsilon_2\sigma_2^\alpha)\right]. \end{aligned} \quad (19)$$

The last term takes into account the missing field on former boundary spins σ_1^α and σ_2^α which are now summed up. It is useful to introduce the operator $1 = \sum_{k=0}^{4n_r} \delta_{k,k_1+k_2+k_3+k_4}$ or the integral form

$$1 = \sum_{k=0}^{4n_r} \delta_{k,k_1+k_2+k_3+k_4} = \sum_{k=0}^{4n_r} \int_0^{2\pi} \frac{d\theta}{2\pi} e^{i\theta(-k+k_1+k_2+k_3+k_4)} \quad (20)$$

which is then inserted in the previous expression in order to reorganize the sum over the k_i into a single sum over weights $x^k(1-x)^{4n_r-k}C_{4n_r}^k$. The integral over θ can be performed using a first order expansion in n , sufficient to obtain $z'_r(0)$. For example, given integer $p > 1$ and $0 \leq k \leq pn_r$, let us consider $n_r + 1$ field variables φ_l and define the quantity $W_{n,k}[\varphi_l]$ made of the product of p sums $\sum_{k_i} C_{n_r}^{k_i} \exp(n\varphi_{k_i})$, $i = 1, \dots, p$ by analogy with the product of sums that appears in (19). In addition, we impose the constraint $\sum_{i=1}^p k_i = k$ by using the Kronecker integral (20), and perform an expansion at first order in n

$$\begin{aligned} W_{n,k}[\varphi_l] &:= \int_0^{2\pi} \frac{d\theta}{2\pi} e^{-i\theta k} \prod_{i=1}^p \left(\sum_{k_i=0}^{n_r} C_{n_r}^{k_i} e^{i\theta k_i + n\varphi_{k_i}} \right) \\ &\simeq \int_0^{2\pi} \frac{d\theta}{2\pi} e^{-i\theta k} \prod_{i=1}^p \left[(1 + e^{i\theta})^{n_r} + n \sum_{k_i} C_{n_r}^{k_i} e^{i\theta k_i} \varphi_{k_i} \right] \\ &\simeq \int_0^{2\pi} \frac{d\theta}{2\pi} e^{-i\theta k} (1 + e^{i\theta})^{pn_r} \left[1 + np(1 + e^{i\theta})^{-n_r} \sum_{k_1} C_{n_r}^{k_1} e^{i\theta k_1} \varphi_{k_1} \right] \\ &= C_{pn_r}^k + np \sum_{k_1} C_{n_r}^{k_1} C_{(p-1)n_r}^{k-k_1} \varphi_{k_1} \simeq C_{pn_r}^k \exp \left(np \sum_{k_1=\max(0,k-(p-1)n_r)}^{\min(k,n_r)} \frac{C_{n_r}^{k_1} C_{(p-1)n_r}^{k-k_1}}{C_{pn_r}^k} \varphi_{k_1} \right). \end{aligned} \quad (21)$$

The exponentiation in the last line allows us, at first order in n , to reorganize the product of the $p = 4$ sums in (5) as a single sum over configurations of k vacant sites, with combinatorial factor $C_{pn_r}^k$. In particular, taking a constant value $\varphi_l := \varphi$, we easily find $W_{n,k}[\varphi] = C_{pn_r}^k e^{np\varphi}$, and therefore the identity

$$\sum_{k_1=\max(0,k-(p-1)n_r)}^{\min(k,n_r)} \frac{C_{n_r}^{k_1} C_{(p-1)n_r}^{k-k_1}}{C_{pn_r}^k} = 1 \quad (22)$$

from which we deduce that factors

$$\mathcal{D}_{n_r,p}^{k,k_1} := \frac{C_{n_r}^{k_1} C_{(p-1)n_r}^{k-k_1}}{C_{pn_r}^k} \quad (23)$$

can be considered as natural weights since the sum over integers k_1 is normalized. We may apply this technique to spin operators $\sum_\alpha \sigma^\alpha \sigma'^\alpha$ appearing in (19) as well,

which are sum of n terms. Considering for example linear spin operator $\sum_{\alpha} \sigma^{\alpha}$, and instead of (21) the function

$$\begin{aligned} W_{n,k}[\varphi_l] &:= \text{Tr} \sigma^{\alpha} \int_0^{2\pi} \frac{d\theta}{2\pi} e^{-i\theta k} \prod_{i=1}^p \left(\sum_{k_i=0}^{n_r} C_{n_r}^{k_i} e^{i\theta k_i + \varphi_{k_i} K \sum_{\alpha} \sigma^{\alpha}} \right) \\ &= \int_0^{2\pi} \frac{d\theta}{2\pi} e^{-i\theta k} \sum_{\{k_i\}} \left(\prod_{i=1}^p C_{n_r}^{k_i} \right) e^{i\theta \sum_i k_i} 2^n \cosh^n \left(K \sum_i \varphi_{k_i} \right). \end{aligned} \quad (24)$$

We then take the limit $n \rightarrow 0$ and define $w_k[\varphi_l] := \partial W_{n,k}[\varphi_l] / \partial n|_{n=0}$, so that

$$w_k[\varphi_l] = \sum_{\sum_i k_i = k} \left(\prod_{i=1}^p C_{n_r}^{k_i} \right) \ln \left[2 \cosh \left(K \sum_i \varphi_{k_i} \right) \right]. \quad (25)$$

We can compare this expression with the approximation

$$w_k[\varphi_l] \simeq \tilde{w}_k[\varphi_l] := C_{pn_r}^k \ln \left[2 \cosh \left(pK \sum_{k_1} \mathcal{D}_{n_r,p}^{k,k_1} \varphi_{k_1} \right) \right] \quad (26)$$

coming from the same analysis made in (21), we can discuss two different cases. First, let choose $\varphi_l := \varphi$, both functions w_k and \tilde{w}_k are identical, using the normalization (22). Then, we may try non-constant fields such as $\varphi_l := l\varphi$, which gives after summation the exact result

$$w_k[\varphi_l = l\varphi] = C_{pn_r}^k \ln \left[2 \cosh(kK\varphi) \right], \quad (27)$$

which is also identical to \tilde{w}_k in (26) using equality $\sum_{k_1} \mathcal{D}_{n_r,p}^{k,k_1} k_1 = k/p$. In the more general case, when the arguments $\phi_{l \leq n_r}$ are random variables, we can try to evaluate the accuracy of (26). Let us consider for example a Poisson distribution for the $\varphi_l > 0$, with mean and variance unity, $\text{prob}(\varphi_l) = \exp(-\varphi_l)$, and K fixed. A measure of the accuracy can be given by the relative error function $g(k) := \langle (\tilde{w}_k[\varphi_l] / w_k[\varphi_l] - 1)^2 \rangle^{1/2}$, where the brackets are the average over random realizations. In Fig. 4 is represented $g(k)$ as function of k for $n = 10$ and for different temperatures $1/K$.

Applying (21) for spin operators will be useful to simplify expression (19) and obtain recursive equations in presence of dilution. Computing recursive equations for $H_k^{(r)}(\epsilon, \epsilon')$, $I_k^{(r)}(\epsilon, \epsilon')$, and $K_k^{(r)}$ follows two steps: the integral over variable θ coming from the constraint $k_1 + k_2 + k_3 + k_4 = k$, with $k_i = 0, \dots, n_r$, introduced in (19), is performed using transformation (21) over the different spin operators with $p = 4$. This will allow for the partial summation over spins σ_1^{α} and σ_2^{α} , and averaging over random variables ϵ_1 and ϵ_2 , see Fig. 1(c). We obtain an expression for Z_{r+1} as a summation over configurations $x^{k+l} (1-x)^{4n_r+2-k-l} C_{4n_r}^k C_2^l$, with $4n_r$ sites coming from inside the shaded diamond structures in Fig. 1(c), plus the two sites coming from the integration over ϵ_1

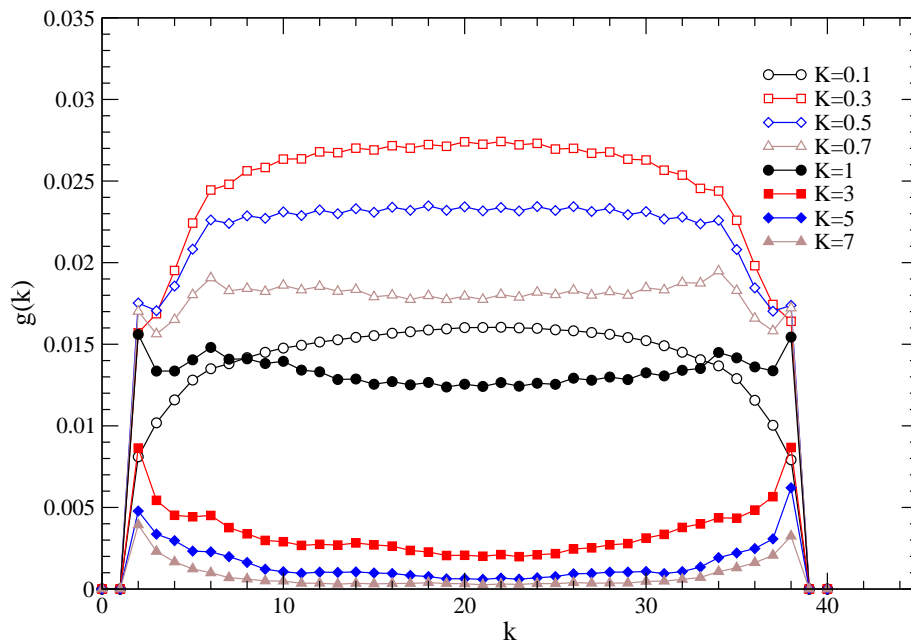


Figure 4. (Color Online) Error function $g(k)$ (see text for definition) that measures the accuracy of the approximation (21) applied to function (24) and performed on random variables φ_l with a Poisson distribution. Here $n_r = 10$ and $0 \leq k \leq 4n_r$, and 15000 realizations were performed before averaging.

and ϵ_2 . This sum can be furthermore reorganized using again identity (21) in order to finally obtain (18) at level $r + 1$ as a sum over weights $x^k(1-x)^{4n_r+2-k}C_{4n_r+2}^k$ (with $4n_r + 2 = n_{r+1}$) and new coupling values. All details of this development are presented in Appendix B, where recurrence equations are written explicitly in (B.11).

Using ansatz (18), and integrating over the boundary site degrees of freedom, the complete partition function (7) is then equal to

$$z_r(n) = \sum_{k=0}^{n_r} C_{n_r}^k x^k (1-x)^{n_r-k} \left[(1-x)^2 \exp(nI_k^{(r)}(1,1)) 2^n \left\{ e^{K_k^{(r)}-K'} \cosh \left[2H_k^{(r)}(1,1) + 2\frac{h_e}{T} \right] + e^{-K_k^{(r)}+K'} \right\}^n \right. \\ \left. + 2x(1-x) \exp(nI_k^{(r)}(0,1)) 2^n \cosh^n \left[H_k^{(r)}(0,1) + \frac{h_e}{T} \right] + x^2 \exp(nI_k^{(r)}(0,0)) \right]$$

and the free energy is derived directly from the previous equation

$$-KF^{(r)} = z_r'(0) = \sum_{k=0}^{n_r} C_{n_r}^k x^k (1-x)^{n_r-k} \left[(1-x)^2 \left\{ \ln(2) + I_k^{(r)}(1,1) \right. \right. \\ \left. \left. + \ln \left(e^{K_k^{(r)}-K'} \cosh \left[2H_k^{(r)}(1,1) + 2\frac{h_e}{T} \right] + e^{-K_k^{(r)}+K'} \right) \right\} \right. \\ \left. + 2x(1-x) \left\{ \ln(2) + I_k^{(r)}(0,1) + \ln \cosh \left[H_k^{(r)}(0,1) + \frac{h_e}{T} \right] \right\} + x^2 I_k^{(r)}(0,0) \right]. \quad (28)$$

After a few steps, the number of configurations is growing rapidly, as the number of weights $C_{n_r}^k x^k (1-x)^{n_r-k}$ becomes exponentially large as well as the number of iterative

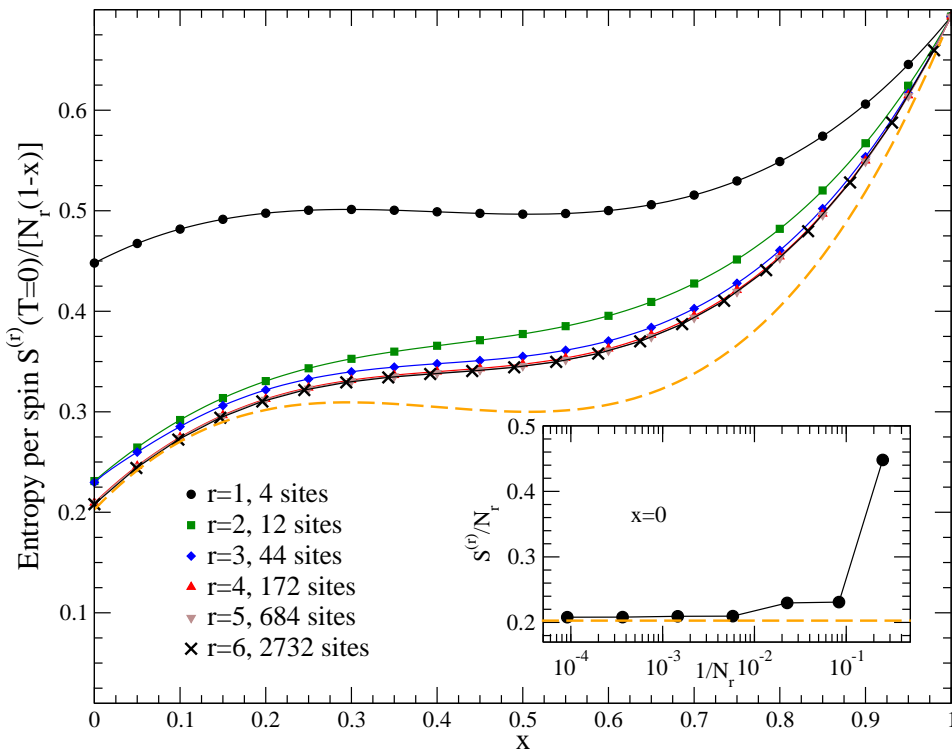


Figure 5. (Color Online) Residual entropy per spin $S^{(r)}/[N_r(1-x)]$ at zero temperature computed from the expression of the free energy (28). The entropy limit per spin for a very dilute system (independent spins) is close to $\ln(2) = 0.6931$ as expected. The orange dashed line represents the Pauling residual entropy $S_P(x)$ given in (30), with a value for the undilute case equal to $S_P(x=0) = \frac{1}{2} \ln(3/2) \simeq 0.2027$ (see text). Inset: zero temperature entropy for the undilute system as function of the inverse system size. First exact values are $S^{(1)}/4 = \ln(6)/4 = 0.4479$, $S^{(2)}/12 = \ln(2)/3 = 0.2310$, $S^{(3)}/44 \simeq 0.2297$. The term at recursion level 6 is approximately equal to $S^{(6)}/2732 \simeq 0.20804$. The dashed straight line is the Pauling entropy $S_P(0)$.

functions to evaluate. We can obtain however a very good approximation if we notice that these weights are distributed closely around a Gaussian when n_r is sufficiently large

$$C_{n_r}^k x^k (1-x)^{n_r-k} \simeq \frac{\exp\left(-\frac{(k-xn_r-x+\frac{1}{2})^2}{2x(1-x)n_r}\right)}{\sqrt{2\pi x(1-x)n_r}} \quad (29)$$

For $r = 4$ for example, the number of internal sites is equal to $n_r = 170$, and the previous approximation is very accurate. Numerically, we solved the iterative functions up to level $r = 4$ included, using (B.11), and then apply for higher levels $r > 4$ the Gaussian approximation for k distributed with 4 standard deviations around the mean value $xn_r + x - 1/2$, which gives precise results.

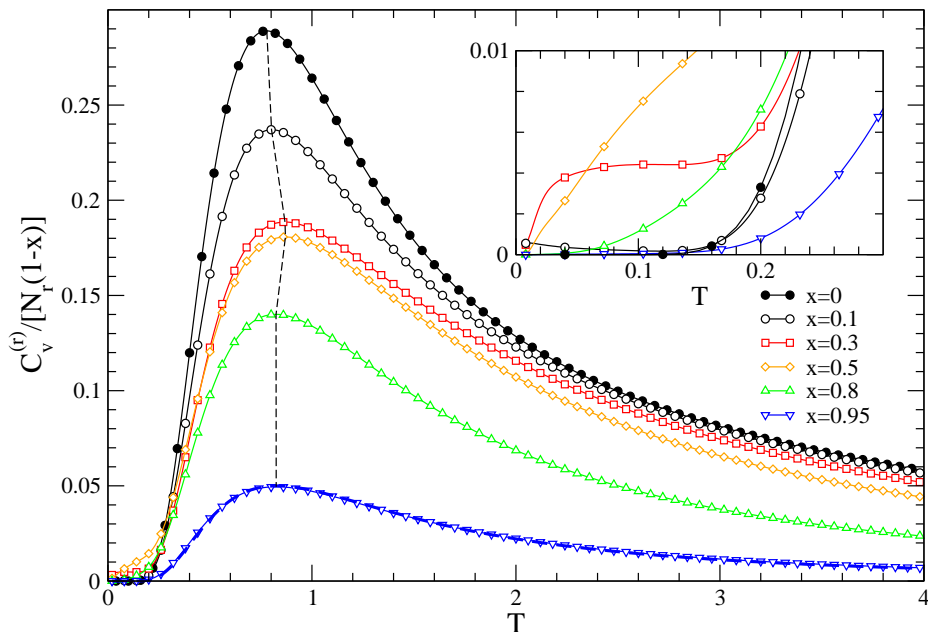


Figure 6. (Color online) Specific heat per spin $C_v^{(r)}/[N_r(1-x)]$ at zero field and level $r = 6$ (2732 sites) for different disorder probability values. Specific heat for the pure case $x = 0$ is derived from the exact recursion equations (A.4) given in Appendix A. The dashed blue line at $x = 0.95$ is the fit with a two-level model which accounts for the Schottky anomaly at a temperature close to unity, see text and (31). Inset: low temperature behavior where a plateau is visible at $x = 0.3$. The dashed black line indicates the position of each Schottky peak as function of dilution.

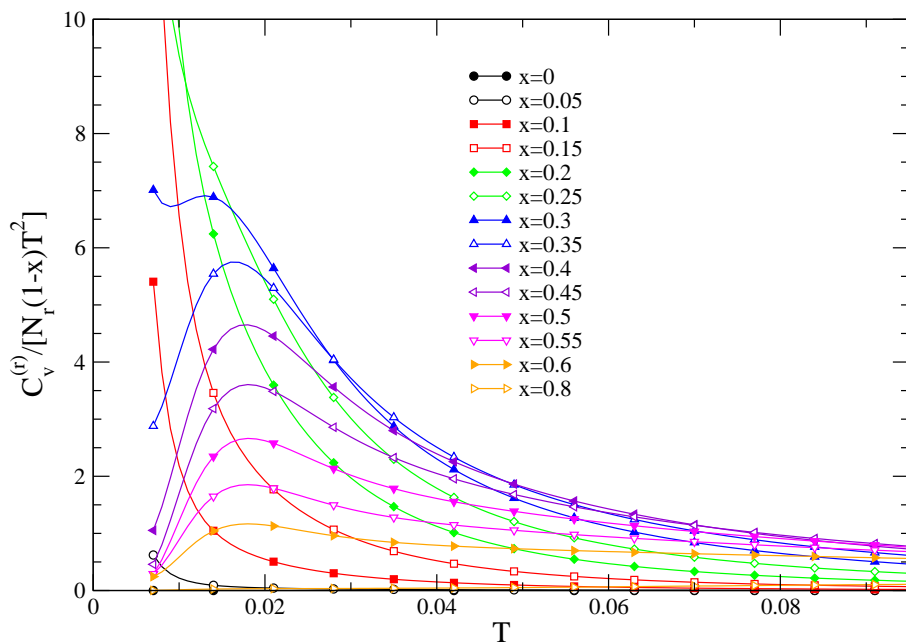


Figure 7. (Color online) Low temperature behavior of specific heat per spin $C_v^{(r)}/[N_r(1-x)T^2]$ at zero field and level $r = 6$ (2732 sites) for different disorder probability values. A local maximum is developing for low dilution $0.1 \leq x \leq 0.3$, then non exponential behavior is observed for intermediate values $x \simeq 0.5$.

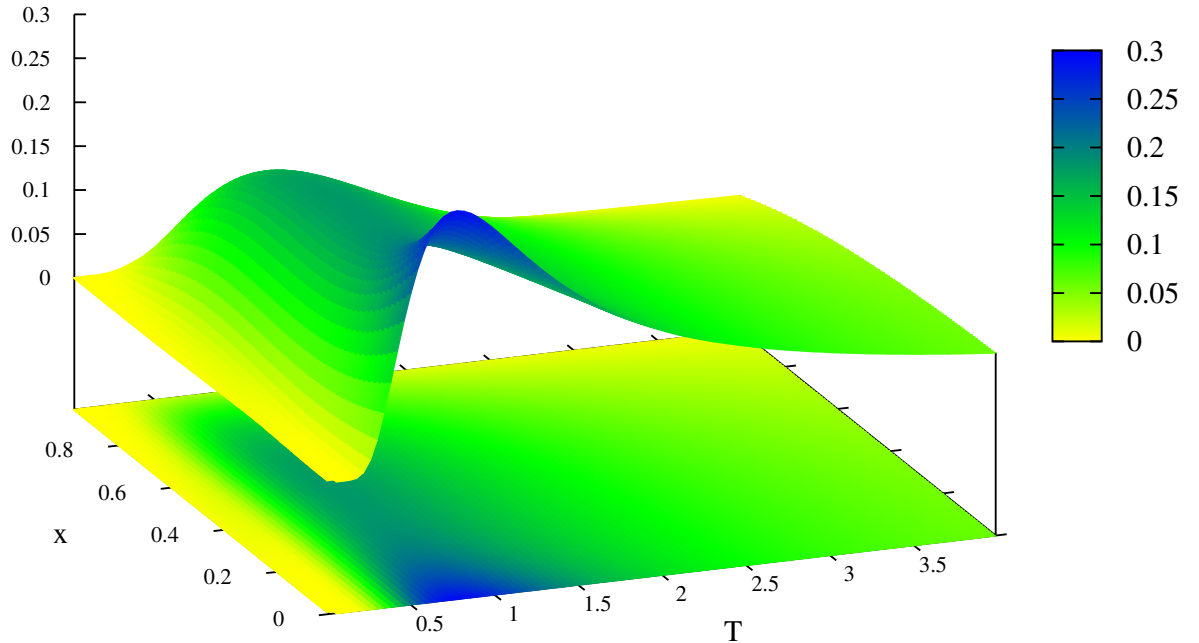


Figure 8. (Color online) Surface plot of the specific heat per spin $C_v^{(r)}/[N_r(1-x)]$ at zero field and level $r = 6$ (2732 sites) as function of temperature and dilution factor x . The Schottky peak amplitude is reduced as x increases.

5. Calorimetry and thermodynamical functions in the dilute case

In this section, we evaluate different thermodynamical quantities as function of dilution using (28). The residual entropy per spin is plotted as function of x in Fig. 5 for r between 1 and 6. For the single tetrahedron structure $r = 1$, the entropy is numerically identical to the exact expression (17) and presents non-monotonic dependence with increasing dilution. For r larger, the entropy is reduced, but saturates rapidly after $r = 5$ which corresponds to 684 sites. In the limit of extreme dilution, the entropy per spin is simply equal to $\ln(2)$ as expected. It is interesting to compare the resulting entropy with the Pauling estimation S_P for an infinite number of tetrahedra treated as independent as function of dilution [13]

$$S_P(x) = \ln(2) - 3x^2(1-x)\ln(2) - 2x(1-x)^2\ln(4/3) - \frac{1}{2}(1-x)^3\ln(8/3). \quad (30)$$

Comparison between S_P , the experimental data for spin-ice $\text{Dy}_{2-x}\text{Y}_x\text{Ti}_2\text{O}_7$ in figure 4 of reference [13], and $S^{(6)}$ shows very similar values at low and moderate dilution,

especially the entropy difference in the undilute case is quite small, $S_P(0) = \frac{1}{2} \ln(3/2) \simeq 0.2027$ and $S^{(6)}/N_6 \simeq 0.20804$ which is an upper bound (see also inset of Fig. 5). Exact values for the undilute hierarchical structure can be computed up to a certain order but the entropy shows a behavior similar to spin ice models. Approximations on pyrochlore lattice made of Ising antiferromagnet tetrahedra give a closer value around 0.20410 [18].

The specific heat $C_v^{(r)}$ is displayed in Fig. 6 as function of temperature for five different values of x . The curves presents in general a broad maximum or Schottky anomaly at a temperature around $T = 1$ corresponding to the typical coupling $J = 1$ and associated with a crossover between a low temperature spin-ice state and paramagnetic state. The system however stays antiferromagnetic in the low temperature regime but is highly degenerated. The ground state energy per spin can be computed exactly for the first terms in absence of dilution $E^{(1)}/4 = -1/2$, $E^{(2)}/12 = -5/6$, and the limiting value is estimated to be $E^{(r \gg 1)}/N_r \simeq -0.9$ using the recurrence equations in Appendix A. The main peak location behaves non-monotonically with dilution, as for dilute compound $\text{Dy}_{2-x}\text{Y}_x\text{Ti}_2\text{O}_7$ in [13], which results from the non-monotonic fraction of ground states in elementary tetrahedral structures as seen for the entropy. At large dilution, the specific heat can accurately be fitted with a two-level model with gap Δ and constant C_0 , as it can be seen in Fig. 6

$$C_v^{approx} = C_0 \frac{\Delta^2}{T^2} \frac{e^{\Delta/T}}{(1 + e^{\Delta/T})^2}. \quad (31)$$

For example, the curve for $x = 0.95$ was fitted with the previous formula using $C_0 \simeq 0.114$ and $\Delta = 1.988$, which corresponds to the specific heat for a gas of dilute pairs of spins with $C_0 \simeq 2(1-x) = 0.1$ and energy coupling very close to $J = \Delta/2 = 1$. At lower temperature however $T \simeq 0.1$, the specific heat presents a second broad peak at intermediate dilution factor $x \simeq 0.3$ (see inset of Fig. 6 and Fig. 7) which can not be reproduced by a two-level model.

These characteristics are exemplified in Fig. 7 for $T \leq 0.1$. The exponential-like Arrhenius behavior of the pure system seems to evolve to more complex features associated with a very small and broad peak contribution at intermediate dilutions and non-exponential deviations. Arrhenius behavior is then recovered when we approach large dilution modeled by (31). We have actually rescaled the specific heat in Fig. 7 by a factor $1/T^2$, in order to check if excitations like phonons or elastic modes are present in the intermediate dilute regime. In this case $C_v^{(r)}$ should scale like T^d with $d = 2$ in our model for a two-dimensional Debye contribution. Such elastic modes (in the low temperature dynamics of domain walls for example) could result from the non-trivial effect of long range and random distribution of the couplings, due to the additional bonds added at each step of the lattice construction which tend to couple remote spins and induce non-local interactions. This could generate a random distribution of local fields, or small gaps at different scales.

Such scaling was analyzed for example in pyrochlore compound $\text{Bi}_2\text{Ti}_2\text{O}_7$ (with $d = 3$) in order to measure the excess of specific heat due to additional Einstein oscillator

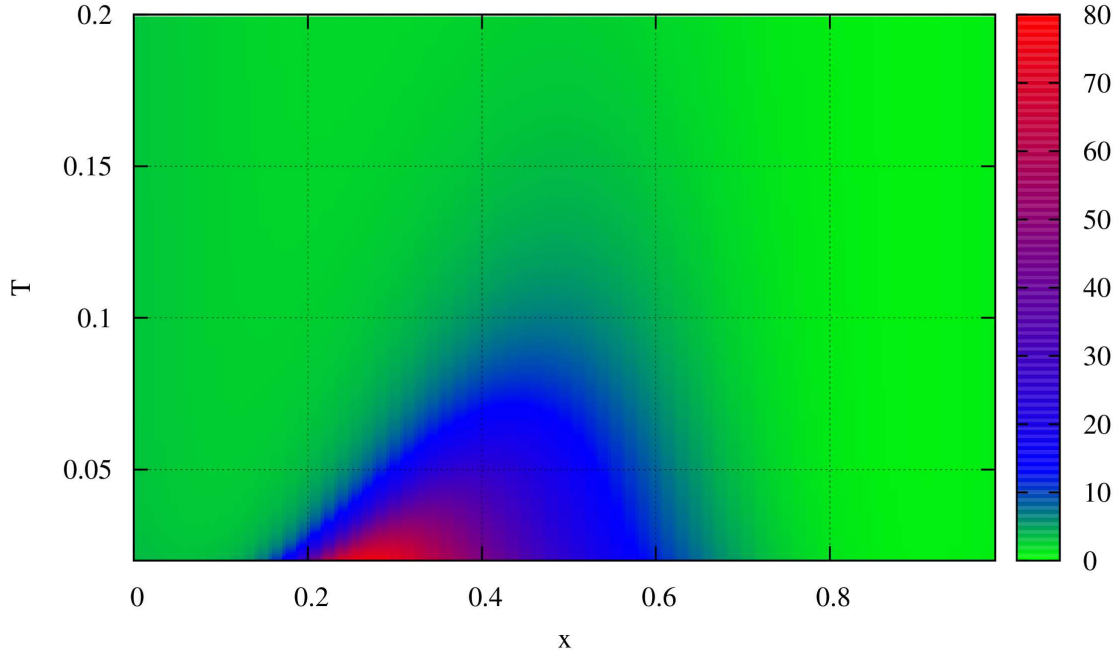


Figure 9. (Color online) Fluctuations Δ_F of the ferromagnetic order parameter M for 2732 sites ($r = 6$) as function of the dilution x and temperature.

contributions that could give rise to a broad peak at low temperature [19]. The scaling in T^2 in Fig. 7 is more appropriate since a T^3 scaling would present clearly a divergence.

Non usual low-temperature specific heat behavior in dilute systems was analyzed, in a different context, for Heisenberg magnets, within the low-temperature spin-wave approximation [20, 21] where dilution induce non trivial temperature exponents depending on the nature of the couplings.

To summarize, the specific heat per spin as function of both temperature T and dilution factor x is displayed in Fig. 8, where the variation of the main Schottky peak amplitude with x shows a decreasing behavior towards a system made of individual pairs of spins with a broader extension.

Fluctuations of the ferromagnetic order parameter defined by $\Delta_F = [\langle M^2 \rangle]_\eta / [(1-x)N_r]$ can be evaluated directly from the free energy using a small field [11]

$$\Delta_F = -\frac{T}{(1-x)N_r} \left. \frac{\partial^2 F^{(r)}}{\partial h_e^2} \right|_{h_e=0} + \frac{1}{(1-x)N_r} \left(\left. \frac{\partial F^{(r)}}{\partial h_e} \right|_{h_e=0} \right)^2 \quad (32)$$

and is plotted in Fig. 9. It takes noticeable values at low temperature for intermediate dilution where short range ferromagnetic order appears to be well

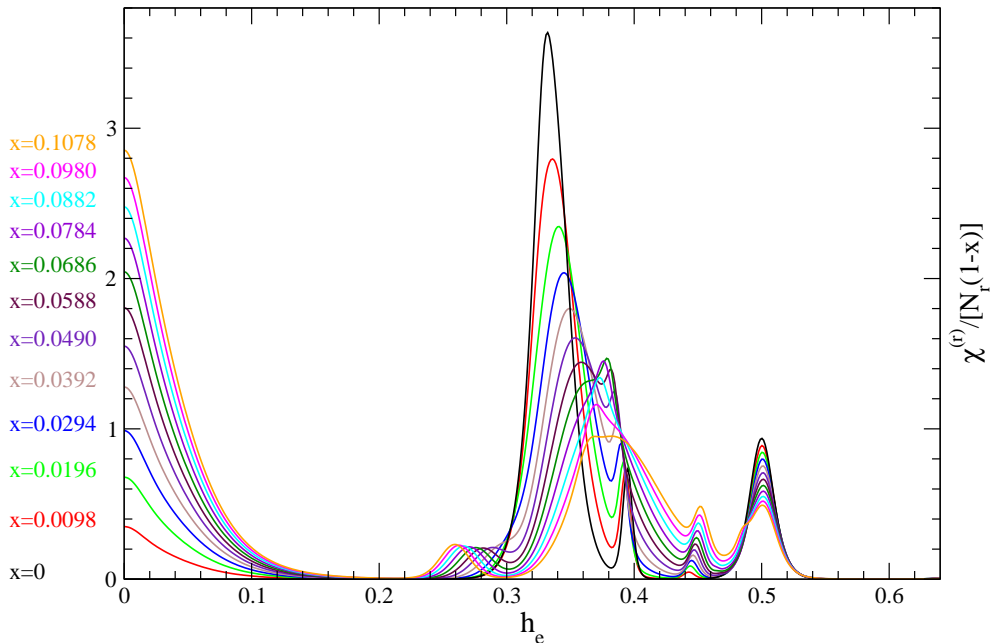


Figure 10. (Color online) Behavior of the susceptibility $\chi^{(r)}/[N_r(1-x)]$ at low temperature ($T=5 \cdot 10^{-2}$) for 2732 sites ($r = 6$) as function of the field h_e and for several dilution factors x . Here are represented only low field excitations $h_e < 0.65$. The values of x are plotted on the left axis with a color corresponding to each curve for clarity.

developed. Such fluctuations could be associated to a classical spin-liquid phase, as opposed to a gas state at higher temperatures [11].

Susceptibility curves as function of dilution and field are plotted in Fig. 10. We chose to represent only the low-field excitations $h_e < 1$ in order to follow the displacement and amplitude of the first peaks with dilution, in particular those corresponding to Fig. 3 in the same low field region. As dilution is increased, a new peak appears at $h_e = 0$ corresponding to excitations of uncoupled and isolated spins. The location of the peak at $h_e = 1/2$ does not change except its amplitude. It is associated to excitations which appear numerically only at recursion level $r = 4$ (172 sites), and might probably consist in flipping two distant spins along the direction of the field, and possibly a series of spin flippings in between, at the cost of one frustrated link only. The energy difference between the two configurations can be written in this case as $\Delta E = 2J - 4h_e$ which is negative when $h_e > 1/2$. Such transition value still persists at low dilution (less than $x = 0.1$), and may result from individual un-dilute structures with the same configurational weight, or configurations.

The peak located at $h_e = 1/3$ which appears at recursion level $r = 3$ is instead moving towards higher field values, with several intermediate peaks in the range $1/5 < h_e < 1/2$. Smaller peaks at $h_e < 1/3$ are moving towards the origin instead. A surface plot Fig. 11 gives a general view of how peaks are moving with field with respect of dilution, and how their amplitude vanishes as we approach the high dilution regime.

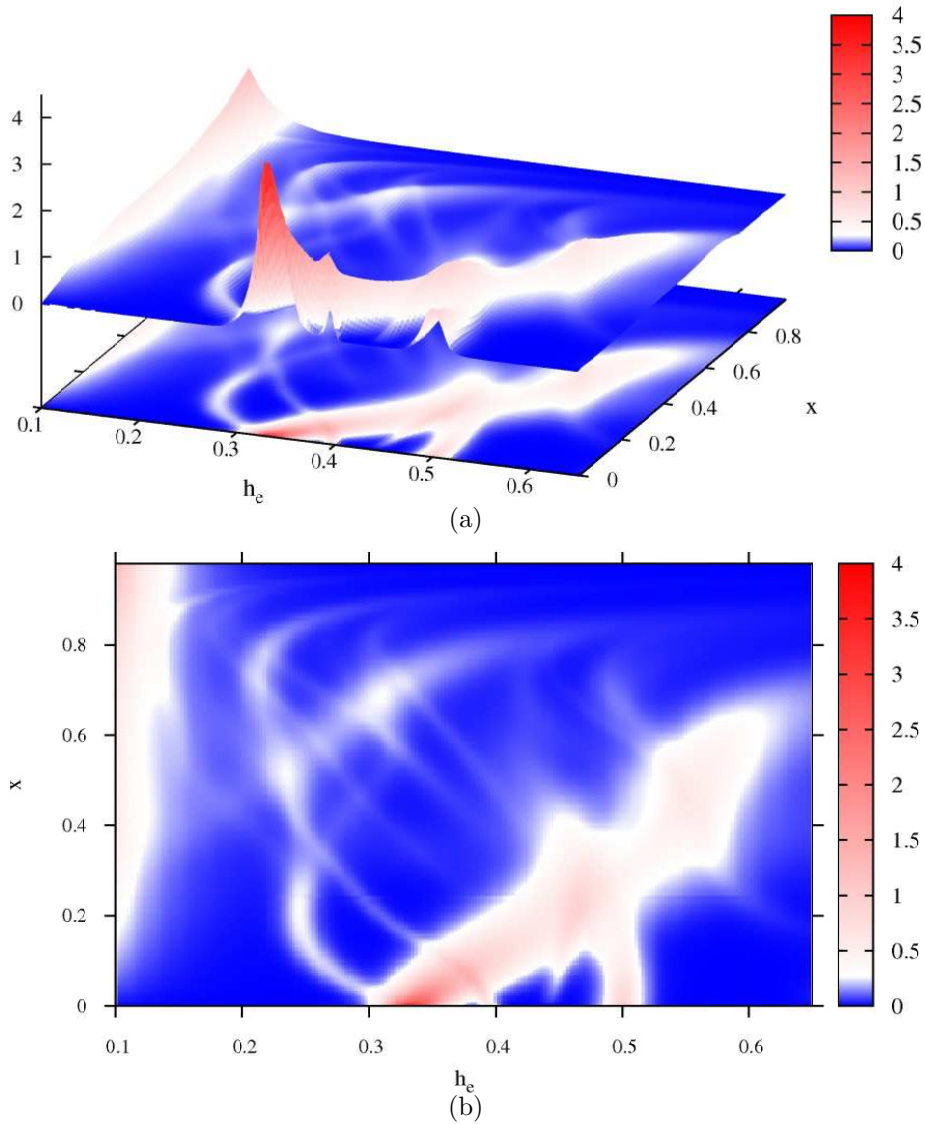


Figure 11. (Color online) (a) Surface plot representing the spin susceptibility $\chi^{(r)}/[N_r(1-x)]$ at low temperature ($T=5 \cdot 10^{-2}$) for 2732 sites ($r = 6$) as function of the field h_e and dilution factors $0 < x < 1$. Here are represented only low field excitations $0.1 < h_e < 0.65$ corresponding to the first three peaks of Fig. 3. (b) Map view of the surface plot.

For higher field, transitions occur in small structures of 4 spins ($r = 1$) where, from a ground state of two spins up and two spins down ($E = -2J$), transitions occur at fields $h_e = 1$ and $h_e = 3$ for spin flip processes corresponding successively to configurations with three spins up, one spin down, and all spins up.

6. Conclusion

In this paper we propose a method to study frustrated hierarchical lattices in presence of dilution based on the replica method and reorganization of configurational weights at

first order in the replica parameter n . Interesting properties of the dilute spin-ice state at low temperature can be examined within this approximation by implementing recursive equations for the partition function and leading to specific heat and susceptibility as function of temperature and external field. Clear crossover evidence is seen between spin-ice and paramagnetic states in the specific heat with the presence of a Schottky peak, and the zero-temperature entropy follows closely the Pauling approximation at least at moderate dilution. Specific heat presents also a secondary contribution at low dilution ($x \sim 0.3$) and very low temperature with non-Arrhenius behavior, at least at the temperatures considered numerically. This feature is probably due to the effect of dilution on the long-range couplings across the lattice, which involves a bimodal distribution of random antiferromagnetic couplings between sites at different scales, and a broad distribution of random effective fields or small gaps.

This makes this hierarchical model a good candidate for exploring in details the physics of spin-ices or spin-liquids. Additional analysis can probably be made using correlation functions for example or short range ferromagnetic order parameter [11] to probe the spin correlations in the low temperature state. This approximation scheme based on replica may probably be implemented more easily to hierarchical spin glass models with modal distribution of couplings, since the quenched disorder is treated as independent between the recursive diamond structures, making the need of a partial partition function not necessary and therefore simplifying the analytical recurrence. We would like to acknowledge M. Gingras for useful discussions on thermal properties in spin-ice systems.

Appendix A. Recursion relations for the non-disordered model

In this appendix we write the recursion relations for the non-disordered case ($x = 0$). Starting from the partition function $Z_0(\sigma, \sigma') = \exp(-K\sigma\sigma')$ of a single antiferromagnetic link between two spins σ and σ' , and $K' = K$, we can generally assume the following recursive and stable form at any step r

$$Z_r(\sigma, \sigma') = \exp\left(I_r - K_r\sigma\sigma' + H_r(\sigma + \sigma')\right) \quad (\text{A.1})$$

with $I_0 = 0$, $K_0 = K$, and $H_0 = 0$ as initial conditions. At the next level $r + 1$, we form the product

$$\begin{aligned} Z_{r+1}(\sigma, \sigma') &= \text{Tr}_{\sigma_1, \sigma_2} Z_r(\sigma, \sigma_1) Z_r(\sigma_1, \sigma') Z_r(\sigma, \sigma_2) Z_r(\sigma_2, \sigma') \\ &\times \exp\left(-K\sigma\sigma' - K\sigma_1\sigma_2 + \frac{h_e}{T}[\sigma_1 + \sigma_2]\right). \end{aligned} \quad (\text{A.2})$$

After replacing Z_r by its ansatz (A.1), and performing the sum over the internal spin degrees of freedom, we obtain

$$Z_{r+1}(\sigma, \sigma') = \exp\left(4I_r - K\sigma\sigma' + 2H_r(\sigma + \sigma')\right) \left\{ 2 \cosh\left[2K_r(\sigma + \sigma') - 4H_r - 2\frac{h_e}{T}\right] e^{-K} + 2e^K \right\}.$$

The term into bracket $\{\dots\}$ can be rewritten as

$$2 \cosh\left[2K_r(\sigma + \sigma') - 4H_r - 2\frac{h_e}{T}\right] e^{-K} + 2e^K = \exp\left(\tilde{I}_r - \tilde{K}_r\sigma\sigma' + \tilde{H}_r(\sigma + \sigma')\right) \quad (\text{A.3})$$

with the following equations for \tilde{I}_r , \tilde{K}_r and \tilde{H}_r

$$\begin{aligned} \exp(\tilde{I}_r - \tilde{K}_r + 2\tilde{H}_r) &= 2 \cosh\left[4K_r - 4H_r - 2H_r\right] e^{-K} + 2e^K, \\ \exp(\tilde{I}_r - \tilde{K}_r - 2\tilde{H}_r) &= 2 \cosh\left[4K_r + 4H_r + 2H_r\right] e^{-K} + 2e^K, \\ \exp(\tilde{I}_r + \tilde{K}_r) &= 2 \cosh\left[4K_r + 2H_r\right] e^{-K} + 2e^K. \end{aligned}$$

This set of equations can be solved by eliminating successively the arguments in the exponential terms. Then the recursive solutions for the new couplings of Z_{r+1} are given by

$$I_{r+1} = 4I_r + \tilde{I}_r, \quad K_{r+1} = K + \tilde{K}_r, \quad H_{r+1} = 2H_r + \tilde{H}_r. \quad (\text{A.4})$$

These relations can be easily implemented in order to compute numerically the different thermodynamical quantities from free energy $F_r = -T \ln Z_r$.

Appendix B. Recursion relations at finite temperature

In this section the recursive equations for the different couplings in (18) are derived. Using Kronecker integral (20), we can rewrite Z_{r+1} as

$$\begin{aligned} Z_{r+1} &= \sum_{k=0}^{4n_r} x^k (1-x)^{4n_r-k} \int P(\epsilon_1)P(\epsilon_2)d\epsilon_1d\epsilon_2 \text{Tr} \sigma_1^\alpha, \sigma_2^\alpha 2^{n(\epsilon_1-1)} 2^{n(\epsilon_2-1)} \\ &\times \exp\left(-K'\epsilon\epsilon' \sum_{\alpha} \sigma^\alpha \sigma'^\alpha - K'\epsilon_1\epsilon_2 \sum_{\alpha} \sigma_1^\alpha \sigma_2^\alpha - K' \sum_{\alpha} (\epsilon_1\sigma_1^\alpha + \epsilon_2\sigma_2^\alpha)(\epsilon\sigma^\alpha + \epsilon'\sigma'^\alpha)\right) \\ &\times \exp\left[\frac{h_e}{T} \sum_{\alpha} (\epsilon_1\sigma_1^\alpha + \epsilon_2\sigma_2^\alpha)\right] \int_0^{2\pi} \frac{d\theta}{2\pi} e^{-i\theta k} \sum_{k_1, k_2, k_3, k_4=0}^{n_r} C_{n_r}^{k_1} C_{n_r}^{k_2} C_{n_r}^{k_3} C_{n_r}^{k_4} e^{i\theta(k_1+k_2+k_3+k_4)} \\ &\times \exp\left\{nI_{k_1}^{(r)}(\epsilon, \epsilon_1) + nI_{k_2}^{(r)}(\epsilon_1, \epsilon') + nI_{k_3}^{(r)}(\epsilon, \epsilon_2) + nI_{k_4}^{(r)}(\epsilon_2, \epsilon')\right. \\ &+ K_{k_1}^{(r)}\epsilon\epsilon_1 \sum_{\alpha} \sigma^\alpha \sigma_1^\alpha + K_{k_2}^{(r)}\epsilon_1\epsilon' \sum_{\alpha} \sigma_1^\alpha \sigma'^\alpha + K_{k_3}^{(r)}\epsilon\epsilon_2 \sum_{\alpha} \sigma^\alpha \sigma_2^\alpha + K_{k_4}^{(r)}\epsilon_2\epsilon' \sum_{\alpha} \sigma_2^\alpha \sigma'^\alpha \\ &+ H_{k_1}^{(r)}(\epsilon, \epsilon_1) \sum_{\alpha} (\epsilon\sigma^\alpha + \epsilon_1\sigma_1^\alpha) + H_{k_2}^{(r)}(\epsilon', \epsilon_1) \sum_{\alpha} (\epsilon'\sigma'^\alpha + \epsilon_1\sigma_1^\alpha) \\ &\left. + H_{k_3}^{(r)}(\epsilon, \epsilon_2) \sum_{\alpha} (\epsilon\sigma^\alpha + \epsilon_2\sigma_2^\alpha) + H_{k_4}^{(r)}(\epsilon', \epsilon_2) \sum_{\alpha} (\epsilon'\sigma'^\alpha + \epsilon_2\sigma_2^\alpha)\right\}. \end{aligned} \quad (\text{B.1})$$

Using (21), we can integrate over θ and rewrite (B.1) as

$$\begin{aligned}
Z_{r+1} &= \sum_{k=0}^{4n_r} C_{4n_r}^k x^k (1-x)^{4n_r-k} \int P(\epsilon_1) P(\epsilon_2) d\epsilon_1 d\epsilon_2 \text{Tr} \sigma_1^\alpha, \sigma_2^\alpha 2^{n(\epsilon_1-1)} 2^{n(\epsilon_2-1)} \\
&\times \exp \left(-K' \epsilon \epsilon' \sum_{\alpha} \sigma^\alpha \sigma'^\alpha - K' \epsilon_1 \epsilon_2 \sum_{\alpha} \sigma_1^\alpha \sigma_2^\alpha - K' \sum_{\alpha} (\epsilon_1 \sigma_1^\alpha + \epsilon_2 \sigma_2^\alpha) (\epsilon \sigma^\alpha + \epsilon' \sigma'^\alpha) \right) \\
&+ \sum_{k_1=\max(0,k-3n_r)}^{\min(n_r,k)} n \mathcal{D}_{n_r,4}^{k,k_1} \left[I_{k_1}^{(r)}(\epsilon, \epsilon_1) + I_{k_1}^{(r)}(\epsilon_1, \epsilon') + I_{k_1}^{(r)}(\epsilon, \epsilon_2) + I_{k_1}^{(r)}(\epsilon_2, \epsilon') \right] \\
&+ \sum_{k_1=\max(0,k-3n_r)}^{\min(n_r,k)} \mathcal{D}_{n_r,4}^{k,k_1} K_{k_1}^{(r)} \sum_{\alpha} (\epsilon \sigma^\alpha + \epsilon' \sigma'^\alpha) (\epsilon_1 \sigma_1^\alpha + \epsilon_2 \sigma_2^\alpha) \\
&+ \sum_{k_1=\max(0,k-3n_r)}^{\min(n_r,k)} \mathcal{D}_{n_r,4}^{k,k_1} \sum_{\alpha} \left[H_{k_1}^{(r)}(\epsilon, \epsilon_1) (\epsilon \sigma^\alpha + \epsilon_1 \sigma_1^\alpha) + H_{k_1}^{(r)}(\epsilon', \epsilon_1) (\epsilon' \sigma'^\alpha + \epsilon_1 \sigma_1^\alpha) \right. \\
&\left. + H_{k_1}^{(r)}(\epsilon, \epsilon_2) (\epsilon \sigma^\alpha + \epsilon_2 \sigma_2^\alpha) + H_{k_1}^{(r)}(\epsilon', \epsilon_2) (\epsilon' \sigma'^\alpha + \epsilon_2 \sigma_2^\alpha) \right] + \frac{h_e}{T} \sum_{\alpha} (\epsilon_1 \sigma_1^\alpha + \epsilon_2 \sigma_2^\alpha) \Big]. \tag{B.2}
\end{aligned}$$

Now the sum over intermediate spins σ_1^α and σ_2^α can be performed directly. Let first define intermediate couplings

$$\tilde{K}_k^{(r)} := \sum_{k_1=\max(0,k-3n_r)}^{\min(n_r,k)} \mathcal{D}_{n_r,4}^{k,k_1} K_{k_1}^{(r)} - K', \tag{B.3}$$

and new functions

$$\begin{aligned}
\tilde{I}_k^{(r)}(\epsilon, \epsilon', \epsilon_1, \epsilon_2) &:= \sum_{k_1=\max(0,k-3n_r)}^{\min(n_r,k)} \mathcal{D}_{n_r,4}^{k,k_1} \left[I_{k_1}^{(r)}(\epsilon, \epsilon_1) + I_{k_1}^{(r)}(\epsilon_1, \epsilon') + I_{k_1}^{(r)}(\epsilon, \epsilon_2) + I_{k_1}^{(r)}(\epsilon_2, \epsilon') \right], \\
\tilde{H}_k^{(r)}(\epsilon, \epsilon', \epsilon_1) &:= \sum_{k_1=\max(0,k-3n_r)}^{\min(n_r,k)} \mathcal{D}_{n_r,4}^{k,k_1} \left[H_{k_1}^{(r)}(\epsilon, \epsilon_1) + H_{k_1}^{(r)}(\epsilon', \epsilon_1) \right]. \tag{B.4}
\end{aligned}$$

Then we isolate the part in (B.2) containing only σ_1^α and σ_2^α , and perform the sum:

$$\begin{aligned}
&\text{Tr} \sigma_1^\alpha, \sigma_2^\alpha \exp \left(-K' \epsilon_1 \epsilon_2 \sum_{\alpha} \sigma_1^\alpha \sigma_2^\alpha + \tilde{K}_k^{(r)} \sum_{\alpha} (\epsilon_1 \sigma_1^\alpha + \epsilon_2 \sigma_2^\alpha) (\epsilon \sigma^\alpha + \epsilon' \sigma'^\alpha) \right) \\
&+ \left[\tilde{H}_k^{(r)}(\epsilon, \epsilon', \epsilon_1) + \frac{h_e}{T} \right] \sum_{\alpha} \epsilon_1 \sigma_1^\alpha + \left[\tilde{H}_k^{(r)}(\epsilon, \epsilon', \epsilon_2) + \frac{h_e}{T} \right] \sum_{\alpha} \epsilon_2 \sigma_2^\alpha \\
&= \prod_{\alpha} \left\{ \exp(-K' \epsilon_1 \epsilon_2) 2 \cosh \left[\tilde{K}_k^{(r)} (\epsilon_1 + \epsilon_2) (\epsilon \sigma^\alpha + \epsilon' \sigma'^\alpha) + \left(\tilde{H}_k^{(r)}(\epsilon, \epsilon', \epsilon_1) + \frac{h_e}{T} \right) \epsilon_1 + \left(\tilde{H}_k^{(r)}(\epsilon, \epsilon', \epsilon_2) + \frac{h_e}{T} \right) \epsilon_2 \right] \right. \\
&\left. + \exp(K' \epsilon_1 \epsilon_2) 2 \cosh \left[\tilde{K}_k^{(r)} (\epsilon_1 - \epsilon_2) (\epsilon \sigma^\alpha + \epsilon' \sigma'^\alpha) + \left(\tilde{H}_k^{(r)}(\epsilon, \epsilon', \epsilon_1) + \frac{h_e}{T} \right) \epsilon_1 - \left(\tilde{H}_k^{(r)}(\epsilon, \epsilon', \epsilon_2) + \frac{h_e}{T} \right) \epsilon_2 \right] \right\}. \tag{B.5}
\end{aligned}$$

Next, we perform the integration over ϵ_1 and ϵ_2

$$\begin{aligned}
 Z_{r+1} &= \sum_{k=0}^{4n_r} C_{4n_r}^k x^k (1-x)^{4n_r-k} \exp\left(-K' \epsilon \epsilon' \sum_{\alpha} \sigma^{\alpha} \sigma'^{\alpha}\right) \\
 &\left[(1-x)^2 \exp\left(n I_k(\epsilon, \epsilon', 1, 1) + \tilde{H}_k^{(r)}(1, 1, 1) \sum_{\alpha} (\epsilon \sigma^{\alpha} + \epsilon' \sigma'^{\alpha})\right) \right. \\
 &\times 2^n \prod_{\alpha} \left\{ \exp(-K') \cosh\left[2\tilde{K}_k^{(r)}(\epsilon \sigma^{\alpha} + \epsilon' \sigma'^{\alpha}) + 2\tilde{H}_k^{(r)}(\epsilon, \epsilon', 1) + 2\frac{h_e}{T}\right] + \exp(K') \right\} \\
 &+ 2x(1-x) \exp\left(n I_k(\epsilon, \epsilon', 0, 1) + \tilde{H}_k^{(r)}(1, 0, 1) \sum_{\alpha} (\epsilon \sigma^{\alpha} + \epsilon' \sigma'^{\alpha})\right) \\
 &\times 2^n \prod_{\alpha} \cosh\left[\tilde{K}_k^{(r)}(\epsilon \sigma^{\alpha} + \epsilon' \sigma'^{\alpha}) + \tilde{H}_k^{(r)}(\epsilon, \epsilon', 1) + \frac{h_e}{T}\right] \\
 &\left. + x^2 \exp\left(n I_k(\epsilon, \epsilon', 0, 0) + \tilde{H}_k^{(r)}(0, 0, 1) \sum_{\alpha} (\epsilon \sigma^{\alpha} + \epsilon' \sigma'^{\alpha})\right) \right]. \quad (\text{B.6})
 \end{aligned}$$

We introduce now a set of functions $\{M_{k,l}(\epsilon, \epsilon'), Q_{k,l}, H_{k,l}(\epsilon, \epsilon')\}$ for each of the three terms appearing in the previous expression and proportional to $(1-x)^2$ ($l=0$), $2x(1-x)$ ($l=1$), and x^2 ($l=2$) respectively. The first factor associated with $(1-x)^2$ can be exponentiated such that

$$\begin{aligned}
 &\exp\left(I_k(\epsilon, \epsilon', 1, 1) + \tilde{H}_k^{(r)}(1, 1, 1)(\epsilon \sigma^{\alpha} + \epsilon' \sigma'^{\alpha})\right) \\
 &\times 2 \left\{ \exp(-K') \cosh\left[2\tilde{K}_k^{(r)}(\epsilon \sigma^{\alpha} + \epsilon' \sigma'^{\alpha}) + 2\tilde{H}_k^{(r)}(\epsilon, \epsilon', 1) + 2\frac{h_e}{T}\right] + \exp(K') \right\} \\
 &= : \exp\left(M_{k,0}(\epsilon, \epsilon') + Q_{k,0} \epsilon \epsilon' \sigma^{\alpha} \sigma'^{\alpha} + H_{k,0}(\epsilon, \epsilon')(\epsilon \sigma^{\alpha} + \epsilon' \sigma'^{\alpha})\right). \quad (\text{B.7})
 \end{aligned}$$

Similarly we have for the second term proportional to $2x(1-x)$

$$\begin{aligned}
 &\exp\left(I_k(\epsilon, \epsilon', 0, 1) + \tilde{H}_k^{(r)}(1, 0, 1)(\epsilon \sigma^{\alpha} + \epsilon' \sigma'^{\alpha})\right) 2 \cosh\left[\tilde{K}_k^{(r)}(\epsilon \sigma^{\alpha} + \epsilon' \sigma'^{\alpha}) + \tilde{H}_k^{(r)}(\epsilon, \epsilon', 1) + \frac{h_e}{T}\right] \\
 &=: \exp\left(M_{k,1}(\epsilon, \epsilon') + Q_{k,1} \epsilon \epsilon' \sigma^{\alpha} \sigma'^{\alpha} + H_{k,1}(\epsilon, \epsilon')(\epsilon \sigma^{\alpha} + \epsilon' \sigma'^{\alpha})\right). \quad (\text{B.8})
 \end{aligned}$$

The last term associated with x^2 can be exponentiated using the values $M_{k,2}(\epsilon, \epsilon') := I_k(\epsilon, \epsilon', 0, 0)$, $Q_{k,2} := 0$ and $H_{k,2}(\epsilon, \epsilon') := \tilde{H}_k^{(r)}(0, 0, 1)$. All these functions can be identified in a unique way by using the four possible configurations for σ^{α} and σ'^{α} . Then the partition function can be rewritten as

$$\begin{aligned}
 Z_{r+1} &= \sum_{k=0}^{4n_r} C_{4n_r}^k x^k (1-x)^{4n_r-k} \exp\left(-K' \epsilon \epsilon' \sum_{\alpha} \sigma^{\alpha} \sigma'^{\alpha}\right) \quad (\text{B.9}) \\
 &\times \left[\sum_{l=0}^2 C_2^l x^l (1-x)^{2-l} \exp\left(n M_{k,l}(\epsilon, \epsilon') + Q_{k,l} \epsilon \epsilon' \sum_{\alpha} \sigma^{\alpha} \sigma'^{\alpha} + H_{k,l}(\epsilon, \epsilon') \sum_{\alpha} (\epsilon \sigma^{\alpha} + \epsilon' \sigma'^{\alpha})\right) \right].
 \end{aligned}$$

As before we can expand the exponential terms at first order in n and rearrange the powers in x such that

$$Z_{r+1}(\epsilon\sigma^\alpha, \epsilon'\sigma'^\alpha) = \exp\left(-K'\epsilon\epsilon'\sum_{\alpha}\sigma^\alpha\sigma'^\alpha\right) \sum_{k=0}^{4n_r+2=n_{r+1}} C_{4n_r+2}^k x^k (1-x)^{4n_r+2-k} \times \quad (\text{B.10})$$

$$\exp\left(\sum_{l=\max(0,k-4n_r)}^{\min(2,k)} \frac{C_{4n_r}^{k-l} C_2^l}{C_{4n_r+2}^k} \left[nM_{k-l,l}(\epsilon, \epsilon') + Q_{k-l,l}\epsilon\epsilon'\sum_{\alpha}\sigma^\alpha\sigma'^\alpha + H_{k-l,l}(\epsilon, \epsilon')\sum_{\alpha}(\epsilon\sigma^\alpha + \epsilon'\sigma'^\alpha) \right] \right).$$

From this result, we can deduce finally the recursive equation for the couplings

$$K_k^{(r+1)} = \sum_{l=\max(0,k-4n_r)}^{\min(2,k)} \frac{C_{4n_r}^{k-l} C_2^l}{C_{4n_r+2}^k} Q_{k-l,l},$$

$$I_k^{(r+1)}(\epsilon, \epsilon') = \sum_{l=\max(0,k-4n_r)}^{\min(2,k)} \frac{C_{4n_r}^{k-l} C_2^l}{C_{4n_r+2}^k} M_{k-l,l}(\epsilon, \epsilon'), \quad \text{and}$$

$$H_k^{(r+1)}(\epsilon, \epsilon') = \sum_{l=\max(0,k-4n_r)}^{\min(2,k)} \frac{C_{4n_r}^{k-l} C_2^l}{C_{4n_r+2}^k} H_{k-l,l}(\epsilon, \epsilon'). \quad (\text{B.11})$$

References

- [1] Kaufman M and Griffiths R B 1981 *Phys. Rev. B* **24**(1) 496–498 URL <http://link.aps.org/doi/10.1103/PhysRevB.24.496>
- [2] Griffiths R B and Kaufman M 1982 *Phys. Rev. B* **26**(9) 5022–5032 URL <http://link.aps.org/doi/10.1103/PhysRevB.26.5022>
- [3] Berker A N and Ostlund S 1979 *Journal of Physics C: Solid State Physics* **12** 4961 URL <http://stacks.iop.org/0022-3719/12/i=22/a=035>
- [4] Gülpınar G and Berker A N 2009 *Phys. Rev. E* **79**(2) 021110 URL <http://link.aps.org/doi/10.1103/PhysRevE.79.021110>
- [5] Kaufman M and Griffiths R B 1982 *Phys. Rev. B* **26**(9) 5282–5284 URL <http://link.aps.org/doi/10.1103/PhysRevB.26.5282>
- [6] Iglói F and Turban L 2009 *Phys. Rev. B* **80**(13) 134201 URL <http://link.aps.org/doi/10.1103/PhysRevB.80.134201>
- [7] Nishimori H 1980 *J. Phys. C: Solid State Phys.* **13** 4071–6
- [8] Nobre F D 2001 *Phys. Rev. E* **64** 046108
- [9] Robinson M D, Feldman D P and McKay S R 2011 *Chaos* **21** 037114 URL <http://dx.doi.org/10.1063/1.3608120>
- [10] Nishimori H 1981 *Progress of Theoretical Physics* **66** 1169
- [11] Kobayashi H, Fukumoto Y and Oguchi A 2009 *Journal of the Physical Society of Japan* **78** 074004 URL <http://jpsj.ipap.jp/link?JPSJ/78/074004>
- [12] Chang L J, Su Y, Kao Y J, Chou Y Z, Mittal R, Schneider H, Brückel T, Balakrishnan G and Lees M R 2010 *Phys. Rev. B* **82**(17) 172403 URL <http://link.aps.org/doi/10.1103/PhysRevB.82.172403>
- [13] Ke X, Freitas R S, Ueland B G, Lau G C, Dahlberg M L, Cava R J, Moessner R and Schiffer P 2007 *Phys. Rev. Lett.* **99**(13) 137203 URL <http://link.aps.org/doi/10.1103/PhysRevLett.99.137203>

- [14] Gingras M 2011 Spin Ice *Introduction to Frustrated Magnetism (Springer Series in Solid-State Sciences vol 164)* ed Lacroix C, Mendels P and Mila F pp 293–330 URL <http://lanl.arxiv.org/abs/0903.2772v1>
- [15] Lin T, Ke X, Thesberg M, Schiffer P, Melko R and Gingras M 2013 Non-monotonic residual entropy in diluted spin ice: a comparison between Monte Carlo simulations of diluted dipolar spin ice models and experimental results preprint URL <http://lanl.arxiv.org/abs/1303.7240v1>
- [16] Jaubert L 2009 *Topological constraints and defects in spin ice* Ph.D. thesis ENS Lyon
- [17] Kaufman M and Griffiths R B 1984 *Phys. Rev. B* **30**(1) 244–249 URL <http://link.aps.org/doi/10.1103/PhysRevB.30.244>
- [18] Singh R R P and Oitmaa J 2012 *Phys. Rev. B* **85**(14) 144414 URL <http://link.aps.org/doi/10.1103/PhysRevB.85.144414>
- [19] Melot B C, Tackett R, O'Brien J, Hector A L, Lawes G, Seshadri R and Ramirez A P 2009 *Phys. Rev. B* **79**(22) 224111 URL <http://link.aps.org/doi/10.1103/PhysRevB.79.224111>
- [20] M F Thorpe A R M and Miyazima S 1982 The specific heat of small particles with a size distribution *Excitations in Disordered Systems (NATO Advanced Study Institute Series B: Physics vol 78)* ed Thorpe M F (Plenum, New York) pp 601–612
- [21] McGrun A R and Thorpe M F 1983 *J. Phys. C: Solid State Phys.* **16** 1255–1269